Politecnico di Milano

Master of Science in Space Engineering

Spacecraft Attitude Dynamics Course

Project

Group No. 79

Lugli Arianna (mat.226672)
arianna.lugli@mail.polimi.it

Zannoni Samuele (mat. 226242)
samuele.zannoni@mail.polimi.it

Sferlazzo Davide (mat.103422)
davide.sferlazzo@mail.polimi.it

Vollono Luca (mat.217293)
luca.vollono@mail.polimi.it

Academic Year 2022/2023

Contents

1 Nomenclature

a	semi-major axis	$[km]$
e	eccentricity	$[-]$
Ω	RAAN	$[deg]$
ω	argument of periapsis	$[deg]$
θ	true anomaly	$[deg]$
$\vec{\omega}$	spacecraft angular velocity	$[rad/s]$
$\vec{\mathbf{h}}$	spacecraft angular momentum	$[kg * m^2/s]$
$\vec{\mathbf{M}}$	torque	$[N * m]$
m	spacecraft mass	$[kg]$
I	inertia moment	$[kg * m^2]$
G	Earth's gravitational constant	$[km^3/kg/s]$
R_e	Earth's radius	$[km]$

2 Introduction

The spacecraft chosen is a 12U CubeSat, orbiting the Earth along a Low Earth Orbit (LEO). The orbit of the spacecraft STALINK-1053 is taken as a reference.

a $[Km]$	e $[-]$	i $[deg]$	Ω $[deg]$	ω $[rad]$	θ $[rad]$
6921	0.0001824	53.0545	37.8515	45.9004	0

Table 1: Orbital Parameters

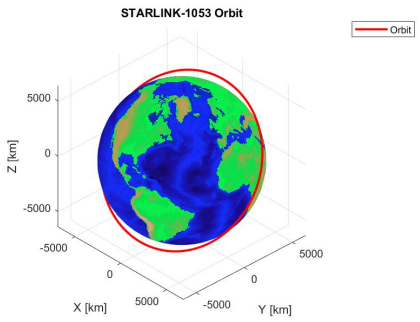

Figure 1: The spacecraft's orbit

The main aim of the CubeSat is to continuously point toward the Earth one of its surfaces, to transmit data without interruption. In order to do so, the spacecraft is equipped with actuators to tackle environmental disturbances and sensors to determine its attitude along the orbit. Furthermore, it has to successfully accomplish a detumbling manoeuvre to neutralize any spinning after the deployment from the launcher.

Here below the spacecraft's main body data are available:

$base$ $[m]$	$height$ $[m]$	$mass$ $[kg]$	I_x $[m^2 * kg]$	I_y $[m^2 * kg]$	I_z $[m^2 * kg]$
0.1	1.2	12	4.32	4.32	0.03

Table 2: Spacecraft Main Body Characteristics

The CubeSat is equipped with two solar arrays placed on the transversal axis, which are able to deploy after the detubling phase. Their characteristics are contained in the table below:

$length$ $[m]$	$height$ $[m]$	$mass/surface$ $[kg/m^2]$	I_x $[m^2 * kg]$	I_y $[m^2 * kg]$	I_z $[m^2 * kg]$
5	1	1.76	440	4.4	440

Table 3: Spacecraft Solar Panels Characteristics

3 ADCS Architecture

An overview of the whole system, including the installed actuators and sensors, is represented below.

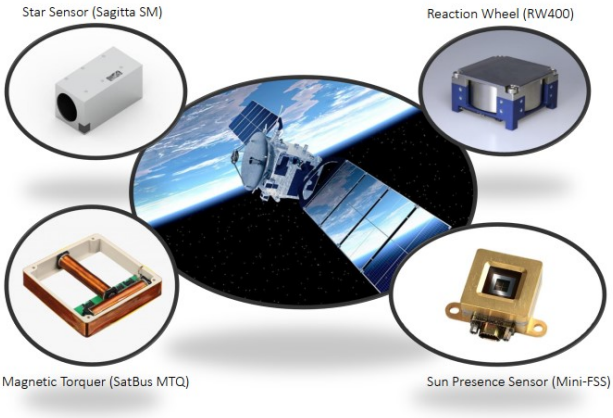

Figure 2: ADCS architecture

4 Description of the Model

4.1 Spacecraft Dynamics

The spacecraft dynamics are described through the integration of the Euler equations in the body frame:

$$[I]\dot{\underline{\omega}} = [I]\underline{\omega} \times \underline{\omega} + \underline{M} \tag{1}$$

In the equation above, [I] is the inertia matrix of the spacecraft, including the inertia of the solar panels, and $\underline{M}$ is the net torque acting on the spacecraft. In particular, the latter is given by the sum of the control and external torque due to environmental disturbances.

With the assumption that the body axes and the principal inertia axes are coincident, it is possible to further develop the Euler equations as below:

$$\begin{cases} \dot{\omega_x} = \dfrac{I_y - I_z}{I_x}\omega_y\omega_z + \dfrac{M_x}{I_x} \\ \dot{\omega_y} = \dfrac{I_z - I_x}{I_y}\omega_x\omega_z + \dfrac{M_y}{I_y} \\ \dot{\omega_z} = \dfrac{I_x - I_y}{I_z}\omega_y\omega_x + \dfrac{M_z}{I_z} \end{cases} \tag{2}$$

4.2 Spacecraft Kinematics

The spacecraft kinematics is described through the use of direction cosines, gathered in the attitude matrix $[A_{B/N}]$. The latter is computed through the integration of the following formula:

$$\frac{d[A_{B/N}]}{dt} = -\begin{bmatrix} 0 & -\omega_3 & \omega_2 \\ \omega_3 & 0 & -\omega_1 \\ -\omega_2 & \omega_1 & 0 \end{bmatrix} \times [A_{B/N}] \tag{3}$$

The orthonormalization of the matrix is ensured by the application of the following iterative formula:

$$[A_{k+1}] = \frac{3}{2} \cdot [A_k] - \frac{1}{2} \cdot [A_k] \cdot [A_k]' \cdot [A_k] \tag{4}$$

In a first-order approximation, it is possible to adopt a single-step iteration as follows:

$$[A_{B/N}] = \frac{3}{2} \cdot [A_0] - \frac{1}{2} \cdot [A_0] \cdot [A_0]' \cdot [A_0] \tag{5}$$

4.3 Spacecraft Orbit

The motion of the spacecraft along its orbit is described through the integration of the true anomaly, according to the Two-Body Problem theory.

$$\dot{\theta} = \frac{n(1 + ecos\theta)^2}{(1 - e^2)^{\frac{3}{2}}} \tag{6}$$

Therefore, it is possible to define the spacecraft orbit in the body frame:

$$\hat{r_B} = [A_{B/N}] \cdot R_orbit \begin{bmatrix} cos(\theta) \\ sin(\theta)cos(i) \\ sin(\theta)sin(i) \end{bmatrix} \tag{7}$$

Furthermore, the direction of the Sun with respect to the spacecraft in the body frame is computed:

$$\hat{S_B} = [A_{B/N}] \cdot R_{Earth-Sun} \begin{bmatrix} cos(n^{Sun}t) \\ sin(n^{Sun}t)cos(\epsilon) \\ sin(n^{Sun}t)sin) \end{bmatrix} \tag{8}$$

5 Environmental Torques

Thanks to the knowledge of the motion of the spacecraft along its orbit, it is possible to carry out an in-depth analysis of the environmental disturbances.

Due to the characteristics of the orbit, the main external torques acting on the spacecraft are the magnetic field torque and the gravity gradient torque.

5.1 Gravity Gradient

The gravity gradient torque has an order of magnitude of $o(10^{-4})$, thus it is the major contributor to environmental disturbances. It is possible to evaluate the net torque acting on an elementary mass in space dm with the following formula:

$$\underline{M_{GG}} = \frac{3Gm_t}{R^5} \int_B (\underline{r} \cdot \underline{R})(\underline{r} \times \underline{R}) dm \tag{9}$$

To evaluate the effect of the gravity gradient torque on the spacecraft dynamics, the Euler equations come in handy:

$$\begin{cases} I_x \dot{\omega_x} + (I_z - I_y)\omega_y \omega_z = \dfrac{3Gm_t}{R^3}(I_z - I_y)c_3 c_2 \\ I_y \dot{\omega_y} + (I_x - I_z)\omega_x \omega_z = \dfrac{3Gm_t}{R^3}(I_x - I_z)c_1 c_3 \\ I_z \dot{\omega_z} + (I_y - I_x)\omega_y \omega_z = \dfrac{3Gm_t}{R^3}(I_y - I_x)c_1 c_2 \end{cases} \tag{10}$$

where the vector $(c_1, c_2, c_3)'$ are the direction cosines of the radial direction in the principal axes.

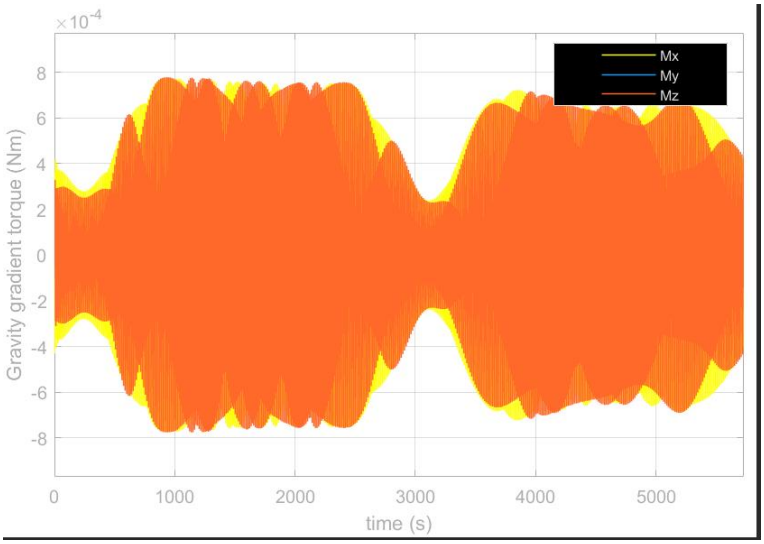

Figure 3: The gravity gradient torque

5.2 Magnetic Field

Due to the low altitude of the orbit, the torque generated by the Earth's magnetic field must be taken into account. To assess the latter torque, the IGRF2000 model (International Geomagnetic Reference Field) has been used. Furthermore, the magnetic field has been modeled as a simple dipole, namely a first-order approximation of the IGRF model, to simplify the computation. However, this model is accurate only for orbits higher than 20000km, thus a more accurate model for the magnetic field should have been implemented. In particular, a model of 13^{th} order must be accurate for such a low-altitude orbit.

The magnetic field in the body frame could be evaluated through the following formula:

$$\underline{b_B} = [A_{B/N}] \cdot \underline{b_N} \tag{11}$$

where $\underline{b_N}$ is the magnetic field in the inertial frame, according to the simple dipole model which follows:

$$\underline{b_N} = \frac{R^3 H_0}{r^3} \cdot [3(\underline{\hat{m}} \cdot \underline{\hat{r}})\underline{\hat{r}} - \underline{\hat{m}}] \tag{12}$$

$$\underline{\hat{m}} = \begin{bmatrix} sin(11.5^{\check{r}})cos(\omega_{Earth}t) \\ sin(11.5^{\check{r}})sin(\omega_{Earth}t) \\ cos(11.5^{\check{r}}) \end{bmatrix} \tag{13}$$

$$H_0 = ((g_1^0)^2 + (g_1^1)^2 + (h_1^1)^2)^{\frac{1}{2}} \tag{14}$$

$$\begin{cases} g_1^0 = -2.9615 \times 10^{-5} T \\ g_1^1 = -1.728 \times 10^{-6} T \\ h_1^1 = 5.186 \times 10^{-6} T \end{cases} \tag{15}$$

A parasitic magnetic torque, which depends on the number of electronic components boarded on the satellite, must be assumed. Even if the CubeSat in the analysis is a small spacecraft, a large $\underline{m}$ is considered to model the controller in the worst-case scenario.

$$\underline{m} = \begin{bmatrix} 0.01 \\ 0.05 \\ 0.01 \end{bmatrix} A \cdot m^2 \tag{16}$$

The torque due to the magnetic field could be found as follows:

$$\underline{M} = \underline{m} \times \underline{b} \tag{17}$$

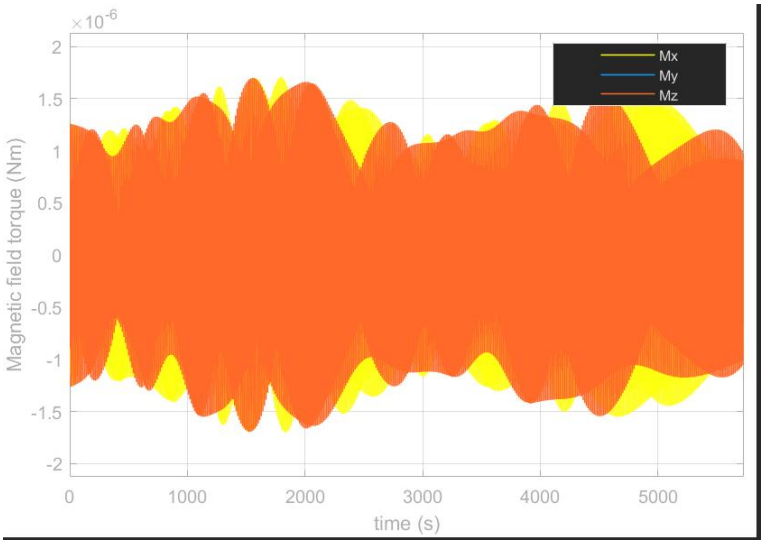

Figure 4: The magnetic field torque

5.3 Aerodynamic Drag and Solar Radiation Pressure

Even if the orbit has a low altitude, the atmospheric drag could be negligible, compared to the other torques, since its order of magnitude is $o(10^{-8})$. The solar radiation pressure torque is not considered because the spacecraft has a long period of shadow when it is not affected by any solar radiation because the Earth blocks the sunlight. As a matter of fact, the solar radiation pressure torque has an order of magnitude of $o(10^{-24})$.

6 Sensors

In order to get a good estimation of its attitude, the spacecraft must be equipped with sensors. In particular, the spacecraft in the analysis is equipped with a star sensor and a Sun presence sensor.

6.1 Star Sensor

The star sensor has to identify the stars in its internal catalog among all the celestial bodies it observes along the orbit. In order to do so, a catalog of stars has been implemented, including the following stars: Altair, Spica, Procyon, Rigel, Betelgeuse, Aldebaran. These stars are selected in different regions of the sky, so as to be able to gain data for the whole orbital period, and with an apparent magnitude limited between 0 and 1, to simplify the identification among all the other visible stars.

The catalog is available in the inertial frame, thus it has to be converted in the body frame to be recognizable by the sensor.

FoV $[deg]$	$Cross-boresight$ ["]	$Around-boresight$ ["]	SBA $[deg]$
25.4 x 25.4	2	10	40

Table 4: SAGITTA Star Tracker Data

Furthermore, a random error is considered along the cross-boresight and the around-boresight direction of the field of view.

6.2 Sun Presence Sensor

The star sensor must be switched off when it points to the Sun since it can damage the sensor. Thus, a Sun-presence sensor is used to determine whether to turn off or not the star sensor. The star sensor is switched off when the radiations coming from the Sun are more inclined than the Sun baffle angle (SBA) of the sensor.

Both the star sensor and Sun sensor are installed on the surface of the spacecraft that points toward deep space.

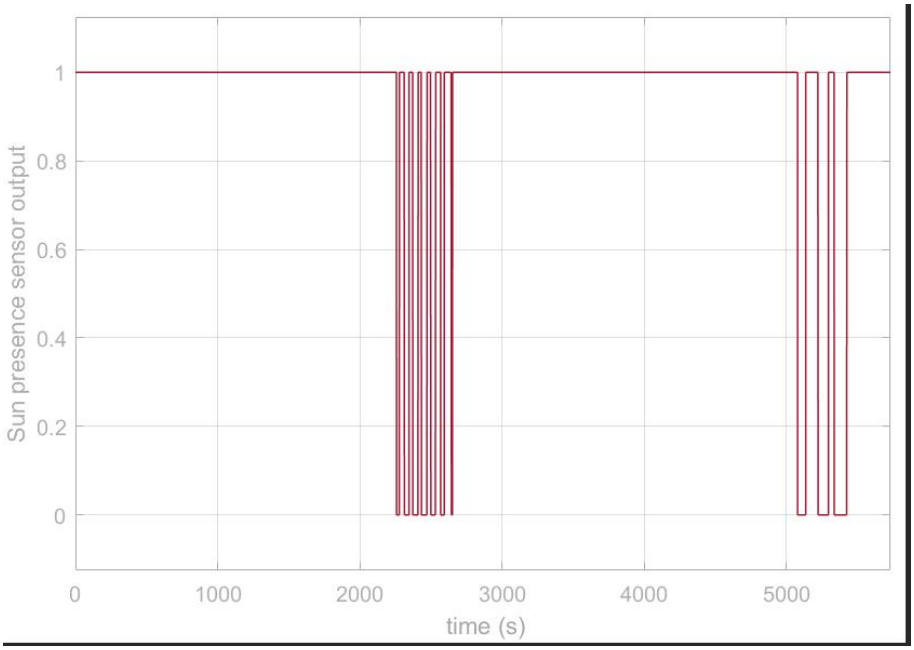

Figure 5: The Sun presence sensor gives a boolean signal as output: 0 if the star sensor is switched off or 1 if the star sensor is switched on

7 Attitude Determination

In order to estimate the attitude from the measurements of the star sensor, a statistical method is used. In particular, the attitude matrix $[A_{B/N}]$ is computed through the analytical solution of Wabha's problem, which consists in minimizing the following function:

$$J([A]) = \frac{1}{2}\sum \alpha_i |s_{Bi} - [A_{B/N}]\nu_{Ni}|^2 \tag{18}$$

where α_i are the weights assigned to the measurements. It's assumed that all the measurements coming from the star sensor have the same weight, set as $1/6$.

Thus, it is possible to compute the attitude matrix $[A_{B/N}]$:

$$[A_{B/N}] = ([B]^T)^{-1}([B]^T[B])^{1/2} \tag{19}$$

where:

$$[B] = \sum \alpha_i s_{Bi} \nu_{Ni}^T \tag{20}$$

8 State Observer

When the star sensor is switched off, the states of the system could not be estimated by the attitude determination method. Thus, a state observer should have been implemented.

9 Control

It is necessary to implement a control logic that makes the satellite able to perform its task, even under the effects of the previous disturbances.

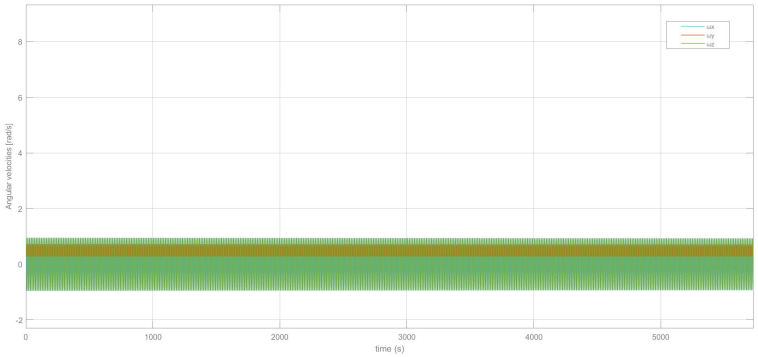

Figure 6: The spacecraft angular velocity without any control implemented.

The spacecraft undergoes three different control phases:

- Detumbling
- Slew maneuver
- Target tracking (Earth-pointing)

A different control approach has been used for each phase.

9.1 Detumbling

The spacecraft is released by the launcher with a certain angular velocity and attitude. The detumbling phase has the aim to completely despin the spacecraft. The angular velocity at the beginning of the detumbling is chosen as follows:

$$\omega_0 = \begin{bmatrix} 0.9 \\ 0.7 \\ 0.3 \end{bmatrix} \tag{21}$$

Since the spacecraft is placed in LEO, a magnetic torquer has been chosen to perform the detumbling. The control logic implemented for this phase is a B-dot proportional control, as follows:

$$\underline{M_c} = -K_b \underline{\dot{B}_m} \times \underline{B} \tag{22}$$

The control torque $\underline{M_c}$ is proportional to the rate of change of the magnetic field in body frame through the gain K_b. Several simulations with different K_b have been carried out to choose the right value.

$$K_b = 1 \times 10^{10} \tag{23}$$

The rate of change of the magnetic field is never aligned with the axes along which the spacecraft spins, thus one magnetic torquer should be sufficient to perform the

detumbling correctly. The rate of change of the magnetic field is estimated by the following formula:

$$\underline{\dot{B_m}} = -\begin{bmatrix} 0 & -\omega_3 & \omega_2 \\ \omega_3 & 0 & -\omega_1 \\ -\omega_2 & \omega_1 & 0 \end{bmatrix} \times \underline{B} \tag{24}$$

The detumbling is carried out approximately for a time of 350 seconds after the spacecraft deployment. During the detumbling all the sensors must be switched off to avoid the generation of parasitic magnetic field.

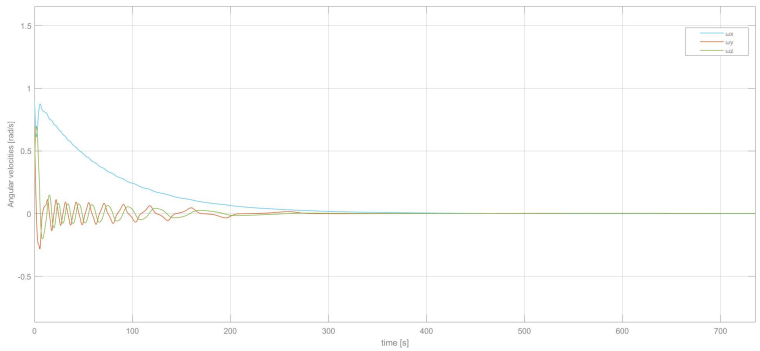

Figure 7: The spacecraft detumbling.

9.2 Slew Manoeuvre

The slew maneuver is performed to move the despun spacecraft toward its desired attitude, so as it can start tracking its target.

When the control torque necessary for the detumbling diminishes below a certain threshold, the slew maneuver is performed. The threshold chosen is the following:

$$\underline{M_c} < 0.001Nm \tag{25}$$

After this threshold, the magnetic torquer is turned off and the reaction wheels and the inertia wheel carry out the slew maneuver.

The control logic chosen for this phase is a PD linear control based on the assessment of the attitude error matrix.

$$[A_{error}] = [A_{B/N}][A_{L/N}]^T = \begin{bmatrix} 1 & a_z & -a_y \\ -a_z & 1 & a_x \\ a_y & -a_x & 1 \end{bmatrix} \tag{26}$$

where $[A_{L/N}]$ is the satellite target attitude matrix and $[A_{B/N}]$ is the satellite attitude matrix measured through the sensors and the attitude determination block.

$$[A_{L/N}] = \begin{bmatrix} cosnt & sinnt & 0 \\ -sinnt & cosnt & 0 \\ 0 & 0 & 1 \end{bmatrix} \tag{27}$$

The control torque obtained is proportional to the attitude error through two assumed gains K_d and K_p.

$$\begin{cases} M_x = K_{px}a_x + K_{dx}\omega_x \\ M_y = K_{py}a_y + K_{dy}\omega_y \\ M_z = K_{pz}a_z + K_{dz}\omega_z \end{cases} \tag{28}$$

$$\underline{k_p} = \begin{bmatrix} 5 \times 10^{-4} \\ 5 \times 10^{-4} \\ 5 \times 10^{-4} \end{bmatrix}; \tag{29}$$

$$\underline{k_d} = \begin{bmatrix} 5 \times 10^{-5} \\ 5 \times 10^{-5} \\ 5 \times 10^{-5} \end{bmatrix}; \tag{30}$$

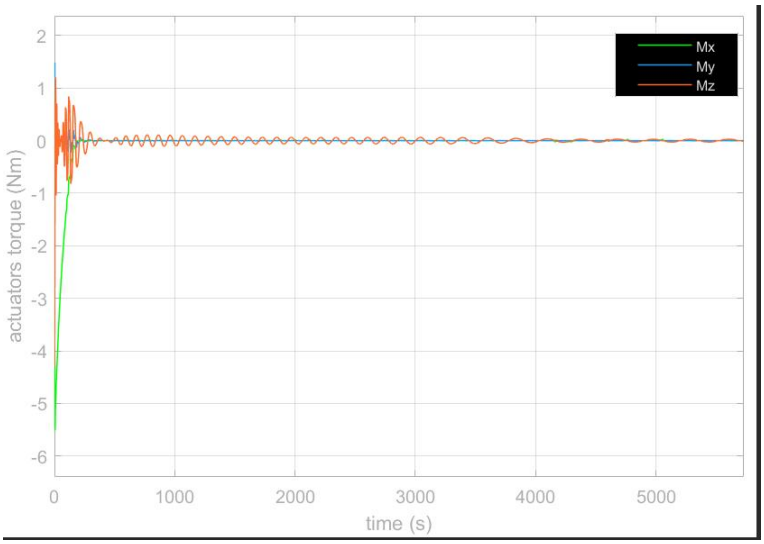

Figure 8: The actuators torque: it's clear that during the detumbling the magnetic torquer applies a strong control torque, while after the detumbling the reaction and the inertia wheel perform the control

9.3 Target Tracking

Target tracking is necessary to keep the spacecraft pointed toward the desired target along its whole orbit.

When the out-of-diagonal terms of the attitude error matrix go below a certain threshold, the control logic switches from the slew maneuver to the target tracking.

$$diag([A_{error}]) < 0.7 \tag{31}$$

The target tracking control follows the same linear PD control logic of the slew manoeuver but with bigger gains to guarantee a small attitude error.

$$\begin{cases} M_x = K_{px}a_x + K_{dx}\omega_x \\ M_y = K_{py}a_y + K_{dy}\omega_y \\ M_z = K_{pz}a_z + K_{dz}\omega_z \end{cases} \tag{32}$$

$$\underline{k_p} = \begin{bmatrix} 5 \times 10^{-2} \\ 5 \times 10^{-2} \\ 5 \times 10^{-2} \end{bmatrix}; \tag{33}$$

$$\underline{k_d} = \begin{bmatrix} 5 \times 10^{-3} \\ 5 \times 10^{-3} \\ 5 \times 10^{-3} \end{bmatrix}; \tag{34}$$

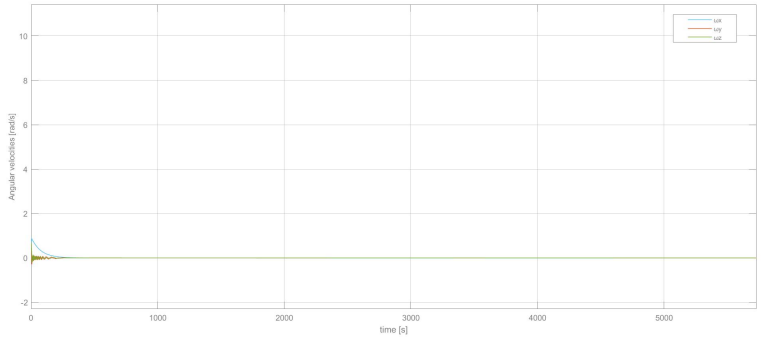

Figure 9: System dynamics with control

10 Conclusion

The spacecraft performs a satisfying detumbling manoeuvre thanks to the magnetic torquer, then it keeps track of the target with success. However, the slew manoeuvre is performed for a very short time (approximately from 350 seconds until 930 seconds after the spacecraft release) because the measured attitude after the detumbling is close to the target attitude of the satellite. The reaction wheels and the inertia wheel doesn't saturate thanks to the use of the magnetic torquer for the detumbling phase.

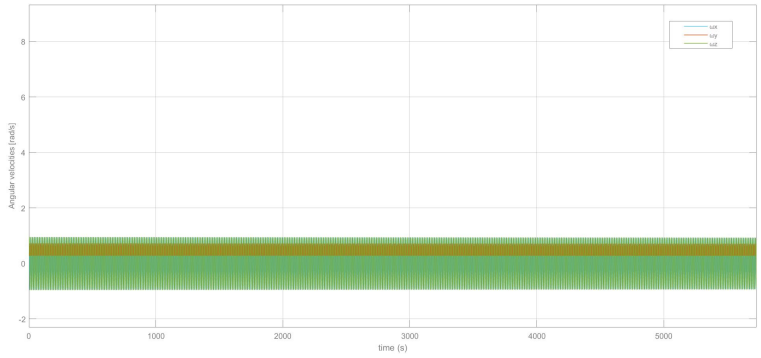

Figure 10: The spacecraft angular velocity without any control implemented.

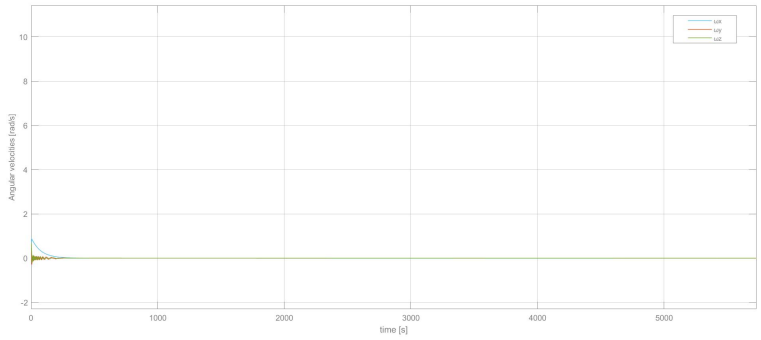

Figure 11: System dynamics with control

11 References

STARLINK-1053 Orbital Data: https://orbit.ing-now.com/satellite/44758/2019-074ax/starlink-1053/
STARLINK-1053 Orbital Data: https://www.n2yo.com/satellite/?s=44758
CubeSat size and mass: https://en.wikipedia.org/wiki/CubeSat
Solar panels size: https://en.wikipedia.org/wiki/Starlink
Solar panels mass: https://www.spectrolab.com/DataSheets/Panel/panels.pdf
Catalogue of stars for the star mapper: Stellarium
SAGITTA SM star tracker data: https://www.cubesatshop.com/product/sagitta-star-tracker/